Removal of copper ions from aqueous solution using low temperature biochar derived from the pyrolysis of municipal solid waste

John Hoslett [a], Heba Ghazal [b], Darem Ahmad [a], Hussam Jouhara [a,*]

[a] College of Engineering, Design and Physical Sciences, Brunel University London, Uxbridge, Middlesex UB8 3PH, UK
[b] School of Pharmacy and Chemistry, Kingston University, Kingston Upon Thames KT1 2EE, UK

HIGHLIGHTS

- Mixed municipal discarded matter (MMDM) removes Cu^{2+} at concentrations >0.005 mol/l.
- MMDM may contain beneficial scrap iron, aiding coagulation/flocculation.
- Iron contamination from char made determining Cu^{2+} sorption capacity difficult.
- SEM-EDAX revealed copper presence in dried biochar after sorption.
- FTIR found differences in functional groups on biochars, particularly paper char.

GRAPHICAL ABSTRACT
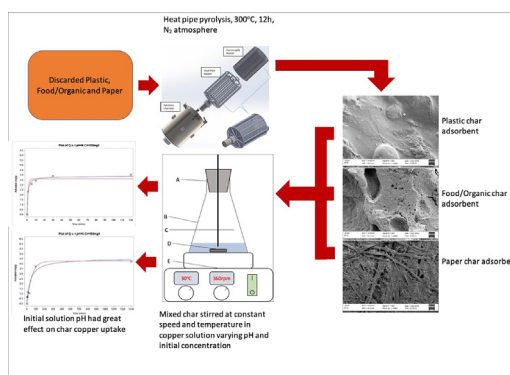
ARTICLE INFO

ABSTRACT

Sustainable methods to produce filter materials are needed to remove a variety of pollutants found in water including organic compounds, heavy metals, and other harmful inorganic and biological contaminants. This study focuses on the removal of Cu(II) from copper aqueous solutions using non-activated char derived from the pyrolysis of mixed municipal discarded materials (MMDM) using a new heat pipe-based pyrolysis reactor. Adsorption experiments were conducted by adding the char to copper solutions of varying concentration (50–250 mg/L) at a constant temperature of 30 °C. The effect of pH on copper adsorption onto the char was also investigated in the range of pH 3 to 6. Copper removal using the char was found to be heavily dependent on pH, adsorption was observed to decrease below a pH of 4.5. However, the initial copper concentration had a little effect on the sorption of copper at high concentration solutions (above 100 mg/L). Overall, the biochar showed an effective copper adsorption capacity (4–5 mg/g) when using copper solutions with a concentration below100 mg/L and pH >4.5. Copper removal using the char tended to follow the pseudo second order kinetic model. Langmuir isothermal model was shown to be the closest fitting isotherm using the linearized Langmuir equation. However, the variety of feedstock used to produce the char led to a variation in results compared to other studies of more specific feedstocks.

© 2019 The Author(s). Published by Elsevier B.V. This is an open access article under the CC BY license (http://creativecommons.org/licenses/by/4.0/).

1. Introduction

Activated carbon (AC) has been used since ancient times in medicinal and water remediation practices. Hippocrates suggested water

* Corresponding author.
  E-mail address: hussam.jouhara@brunel.ac.uk (H. Jouhara).

should be filtered through wood char (González-García, 2018) reducing bad tastes and odours as well as the risk of contracting diseases such as anthrax (González-García, 2018). Typical practices to produce AC include an activation process at high temperature involving chemical or steam treatment and increasing the temperature past 600 °C after pyrolysis. These processes enhance the properties of a pyrolyzed substance.

Some heavy metals such as copper (Cu), chromium (Cr), iron (Fe), magnesium (Mg), and manganese (Mn), are essential micronutrients as they play important biochemical and physiological roles in biological systems at ambient conditions (Singh et al., 2011). Anthropogenic activities have polluted the environment with excess amounts of heavy metals. Metals such as copper are introduced by industrial effluents, mining processes and water pipework (Lone et al., 2008). Heavy metal contamination is mainly due to poor monitoring and waste management processes in developing nations compared to developed nations (da Silva et al., 2018; Idrees et al., 2018; National Research Council, 2000). Copper is a natural element with a widespread distribution, however, exposure to excessive amounts can cause serious health problems because of its bio-accumulation and toxic effects. Heavy metals can be removed by different methods including physico-chemical processes, chemical/electro-chemical processes, coagulation/flocculation, ion exchange, membrane filtration, and biological sorption (Al-Saydeh et al., 2017; Gunatilake, 2015). Adsorption methods have received attention in recent years, with AC adsorbents being produced from fossil fuel materials such as coke, often involving steam and/or metal hydroxide activation (Wu et al., 2018).

With sustainable resources becoming a greater concern in recent decades, research has focused on the production of AC from feedstocks. Pyrolysis of discarded materials such as rice husks, fruit stones, nut shells etc. have been extensively researched (Balasundram et al., 2017; Menya et al., 2018a, 2018b; Momčilović et al., 2011; Satayeva et al., 2018; Spahis et al., 2008). Furthermore, research has shown that certain pyrolysis conditions and feedstocks can have negative net CO_2 emissions compared with other pyrolyzed adsorbent materials (Moreira et al., 2017). The pyrolysis of a specific material and the ability of the produced char to remove aqueous pollutants have also been investigated (El Maguana et al., 2018; Enniya et al., 2018; Marques et al., 2018; Rashidi and Yusup, 2017). There is a wealth of recent articles regarding municipal, industrial and agricultural sewage sludge as a precursor (Al-Malack and Dauda, 2017; Kaçan and Kütahyalı, 2012; J. Li et al., 2018). However, there is a lack of information available on char produced from mixed municipal discarded material (MMDM) as a precursor material and the feasibility of using this char in water purification. Studies that considered MMDM often separated different materials and pyrolyzed at temperatures around 500 °C followed by activation at high temperature, steam, chemical or microwave process (Kumar and Ganesapillai, 2017).

Ho et al. (2017) found that waste activated sludge, and anaerobic digested sludge pyrolyzed between 400 and 800 °C, had greater O/C, and H/C ratio values at lower pyrolysis temperatures rather than at higher pyrolysis temperatures. This is significant as higher O/C and H/C values suggest greater potential for surface complexation of heavy metals. The finding that H/C and O/C values decrease with increasing temperature is corroborated by Qian et al. (2016). Heavy metal sorption to char is a complex process as heavy metals are removed via different mechanisms including surface complexation, electrostatic interaction, cation exchange and precipitation.

Abdelhadi et al. (2017) found that char pyrolyzed at temperature as low as 350 °C had a high affinity towards heavy metals due to the presence of hydroxy, phenolic, carboxylic and methoxy functional groups. Other studies also reported comparable or even favourable removal of transition metal ions using low temperature (300–500 °C) char compared to char pyrolyzed at a higher temperature (Abdelhadi et al., 2017; Luo et al., 2018; Poo et al., 2018). Heavy metals are removed from aqueous solutions in greater amounts by an AC with a more highly

negative surface charge due to electrostatic attraction between positive aqueous heavy metal ions and the surface (Da'na and Awad, 2017). Copper is effectively removed at acidic pH values ranging from 3.5 to 5 (Da'na and Awad, 2017). At higher pH, insoluble copper compounds such as $Cu(OH)_2$ are formed, which limits the interaction and sorption by the char. Research has found that there is little increase in metal removal by chemisorption at pH >5 (Abdelhadi et al., 2017; Zhou et al., 2013).

Mixed municipal discarded material (MMDM) consists of all materials discarded by a household, this includes plastics, organic material, paper, metals, and other materials such as glass. Additionally, the fractions of different materials present in MMDM varies between nations, and regions (Jouhara et al., 2017), with information provided by the World Bank Group (Group, 2012) showing that higher income level nations tend to discard higher proportions of plastics and papers and lesser amounts of organic materials than lower income level nations. Different feedstocks have different adsorption characteristics, thus biochar adsorbents produced from MMDM procured in different income levels may also have varying adsorption capacity (Ahmad et al., 2018; Pellera et al., 2012; Rodríguez-Vila et al., 2018).

The objective of the current study is to examine the feasibility of using char produced from the pyrolysis of MMDM at low temperature (≈300 °C) as an adsorbent for aqueous copper removal. With few articles available regarding the use of mixed feedstocks, the overall purpose of this work is to determine the ability of pyrolyzed, non-activated MMDM to adsorb copper from aqueous solution. The aim is the use of such materials as simple yet effective adsorbents in a developing nation. To the authors' knowledge there are no other articles in existence concerning char derived from a heat pipe-based reactor at 300 °C for use as an adsorbent of heavy metals such as copper ions.

2. Methodology

2.1. Materials

Titripur sulphuric acid and sodium hydroxide, both 0.5 M concentration solution and analytical grade copper (II) sulphate pentahydrate were obtained from Fisher Scientific. Deionised water for the experiments was produced by Vison 250 Deioniser (RS solutions).

2.2. Preparation of char

Pyrex Borosilicate Conical flask (capacity 500 mL) and rubber bung were obtained from Fisher Scientific. A VELP Scientifica AREX Aluminium stirring hotplate was used to stir the char in solution at a constant temperature of 30 °C.

The pyrolysis was performed using a heat-pipe based reactor which provides constant heat flux to the process, described previously by (Jouhara et al., 2018) and illustrated in Fig. 1. MMDM mixture of plastic, meat, paper and other food waste such as bread was fed into the reactor. The pyrolysis retention temperature was set at 300 °C under N_2 atmosphere for 12 h. The collected char was left to cool and then crushed by pestle and mortar. A mechanical sieve was used to separate char powder with a particle size between 3 mm and 250 μm which was used in the current study.

2.3. Copper solutions and adsorption experiments

Solutions of Cu^{2+} ions were prepared by dissolving 12.49 g $CuSO_4.5H_2O$ in 500 mL deionised water to produce a 0.1 M stock solution. The final pH values of the solutions were adjusted to a given pH as outlined in Table 1 using 0.5 M Titripur sulphuric acid or 0.5 M Titripur sodium hydroxide solution.
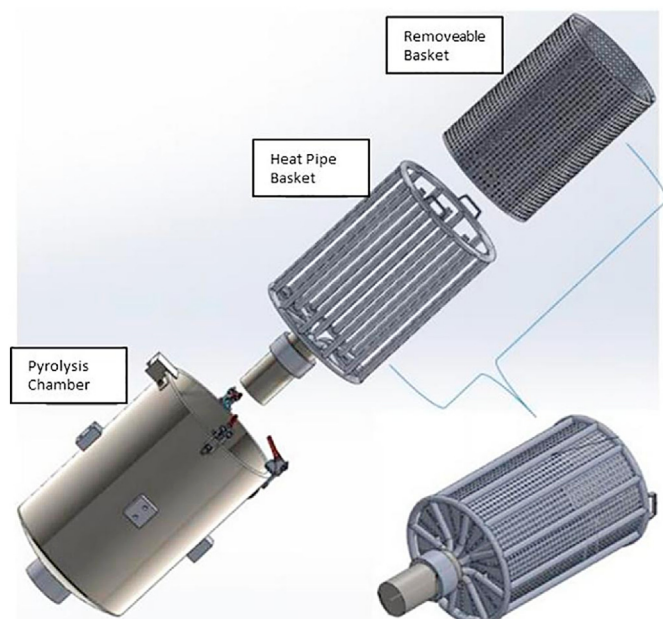
Fig. 1. Schematic drawing of heat pipe based pyrolysis reactor used (Jouhara et al., 2018).

Adsorption experiments were carried out in 500 mL Pyrex Borosilicate conical flask using 100 mL pH adjusted copper sulphate solutions and 0.5 g of char powder. The initial concentration of copper sulphate was between 0 and 250 mg/L and the pH of the initial solution was between 3 and 6, as listed in Table 1. The samples were stirred magnetically at 360 rpm and temperature was maintained at 30 °C using hotplate (A VELP Scientifica AREX). The rubber bung was placed on the neck of the flask to prevent evaporation between sampling (see Fig. 2). Separate experiments were conducted for time intervals of 1, 5, 10, 30, and 120 min for each of the outlined conditions in Table 1. Further 24 h experiments were conducted at pH 5 for the determination of isothermal models. The collected samples were centrifuged at 6000 rpm for 150 s, 14 mL of the supernatant were passed through 0.45 μm Nalgene filter syringes (Thermo Scientific).

This method has been designed in order to explore the effects of pH as well as to determine kinetic and isothermal properties of the char.

The quantity of the copper retained by the char was calculated using the following equation:

$$Q_t = \frac{(C_0 - C_t)V}{M} \tag{1}$$

where Q_t is the adsorption of copper to char at time t (mg/g) Co is the initial concentration of copper (mg/L) and C_t is the concentration at

Table 1
Experimental conditions investigated.

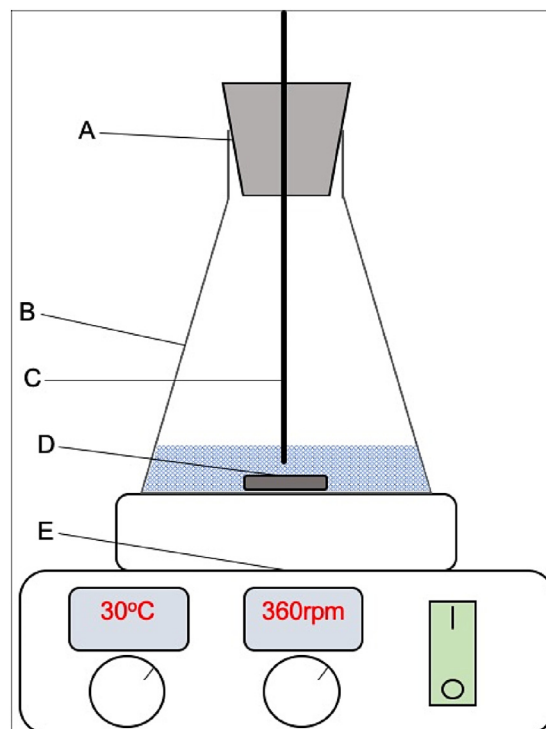| pH	Initial copper concentration (mg/L)
5	50
5	100
5	150
5	200
5	250
5	0
3	150
3.5	150
4	150
4.5	150
5	150
5.5	150
6	150

Fig. 2. Experimental set up of magnetic stirring procedure, (A) denotes the rubber bung in the neck of the conical flask (B), with the temperature control probe (C) inserted through a small hole in the bung, (D) the magnetic stirring pill and (E) the magnetic stirrer plate.

time t (mg/L), V is the volume of solution (l) and M is the mass of the char in solution (g).

2.4. Copper analysis

Copper quantification in the adsorption samples was done using Flame assisted Atomic Absorption Spectrometry (F-AAS) Perkin Elmer AA Analyst 100. A calibration curve of copper sulphate solutions in water was prepared at concentrations of 50, 100, 150, 200, 250 mg/L starting from a stock solution 0.1 M of $CuSO_4 \cdot 5H_2O$. The samples from the adsorption study were diluted prior to analysis using Milli-Q deionised water. All samples were acidified to 5% concentration by volume using 70% concentration, analytical grade nitric acid.

2.5. Char characterization

2.5.1. Scanning electron microscopy-dual energy X-ray absorptiometry (SEM-EDAX)

SEM-EDAX analysis was conducted using a Zeiss Supra SEM with EDAX attachment. Six char samples were explored for their surface morphology as well as elemental composition. Three of these samples were analysed before copper sorption, and three samples afterwards. EDAX was undertaken in triplicate on each SEM image to identify the elemental composition of the scanned sample.

2.5.2. Fourier transmission infra-red (FTIR)

FTIR analysis was carried out on samples of char taken before the addition of copper solution. This was undertaken to determine the functional groups present in chars of different feedstock precursors. In this study char was produced from three groups of material, plastics, food/organic, and paper char, all found in MMDM. It was suspected that chars produced from these different feedstock groups would have different microscopic and chemical characteristics (Pan et al., 2019; Zhang et al., 2017).

2.6. Adsorption kinetics and isotherms

Adsorption Kinetics and isotherms were determined using non-linear regression analysis using SAS University Edition. The method of non-linear regression used was the modified Gauss Newton method. The pseudo first order and pseudo second order kinetic models analysed are displayed in Eqs. (3) and (4) respectively; the Langmuir and Freundlich adsorption isotherms are shown in Eqs. (5) and (6) respectively.

The two benefits of using non-linear regression techniques are that the concentration at equilibrium (C_e) does not need to be known in order to analyse the adsorption kinetics of the char in solution; and error transformations do not occur between linear determined values, and the final non-linear plots as is the case in other studies (Lin and Wang, 2009). Both non-linear models and linear models were conducted on all pH 5 experiments, equilibrium is assumed to be reached in 24 h experiments, as well as any experiment where an equilibrium concentration is reached.

$$Q_e = \frac{(C_i - C_e)V}{m} \tag{2}$$

$$Q_t = Q_{e,PFO}\left(1 - e^{-K_1 t}\right) \tag{3}$$

$$Q_t = \frac{K_2 Q_{e,PSO}^2 t}{1 + K_2 Q_{e,PSO} t} \tag{4}$$

$$Q_e = \frac{C_e K_L Q_m}{1 + (K_L C_e)} \tag{5}$$

$$Q_e = K_f C_e^{1/n} \tag{6}$$

Q_e is the sorption capacity at equilibrium (mg/g), C_i is the initial pollutant concentration (mg/L), C_e is the concentration at equilibrium (mg/L), V is the volume of polluted solution (L), m is the dosage of adsorbent (g/L), $Q_{e,PFO}$ is the adsorption at equilibrium according to the pseudo first order kinetic model, K_1 is the pseudo first order constant, $Q_{e,PSO}$ is the equilibrium adsorption according to the pseudo second order kinetic model, K_2 is the pseudo second order constant ($g\,mg^{-1}\,min^{-1}$), K_L is the Langmuir constant ($L\,mg^{-1}$), Q_m is the maximum sorption capacity in the initial concentration range (mg/g), K_f is the Freundlich constant ($L\,g^{-1}$) and n is the Freundlich intensity constant.

3. Results and discussion

The results section first presents the SEM-EDAX analysis followed by the FTIR to show the varying characteristics between chars produced from different feedstocks, as well as their ability to adsorb copper. Following this, results from the AAS are presented showing the adsorption kinetics and isothermal models of copper to the char. And lastly the effect of pH on the adsorption of copper to MMDM derived char is discussed.

3.1. Char characterization using SEM/EDAX

Fig. 3 A, B and C show SEM images of plastic, food/organic and paper char, respectively. Regarding the plastic char, it is clearly noticeable that its surface is fairly featureless compared to organic and paper chars. Paper char appears to have retained a similar structure to paper precursor material, with latticed fibres clearly visible, this characteristic is not seen in either the plastic or organic chars. The organic char displays a highly varied surface with an apparent significant variation in pore sizes and surface morphology.

Displayed in Fig. 4 A B and C are the SEM images of plastic, food/organic and paper chars, respectively, analysed using energy
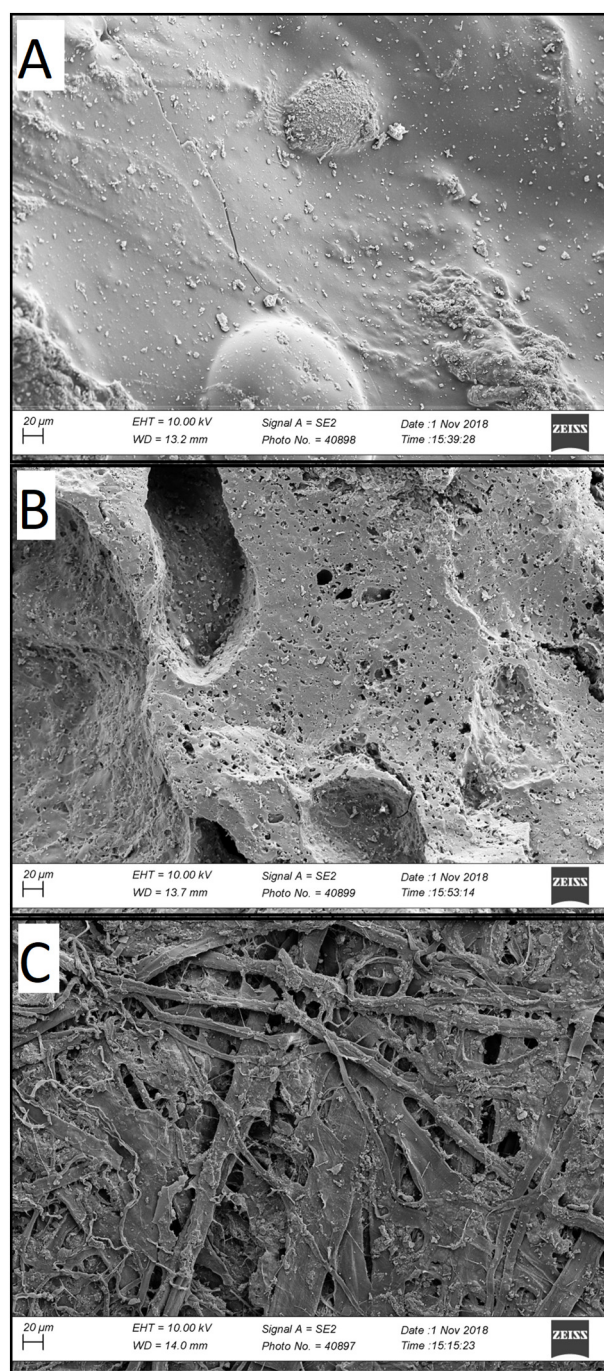

Fig. 3. SEM image of plastic char (A), food/organic char (B), paper char (C), imaged at 500× magnification, at a working distance of 13–14 mm, with an electron energy of 10 kV.

dispersive x-ray analysis (EDAX). Fig. 4 D, E and F show the weight % of each element in each analysis area for plastic, food/organic and paper char, respectively. The final bar on the right of the graphs in Fig. 4 D, E and F show the full area scan with elemental compositional results for each char.

The main element in EDAX scans was carbon. However, the amount was found to vary between paper, plastic and food/organic chars. Paper char displayed the least amount of carbon in its full area scan, with food/organic, and plastic chars displaying similar weight % of carbon in their full area scans. Additionally, elemental composition was found to vary within the full scans, particularly in areas where particles with a crystalline appearance were prevalent.
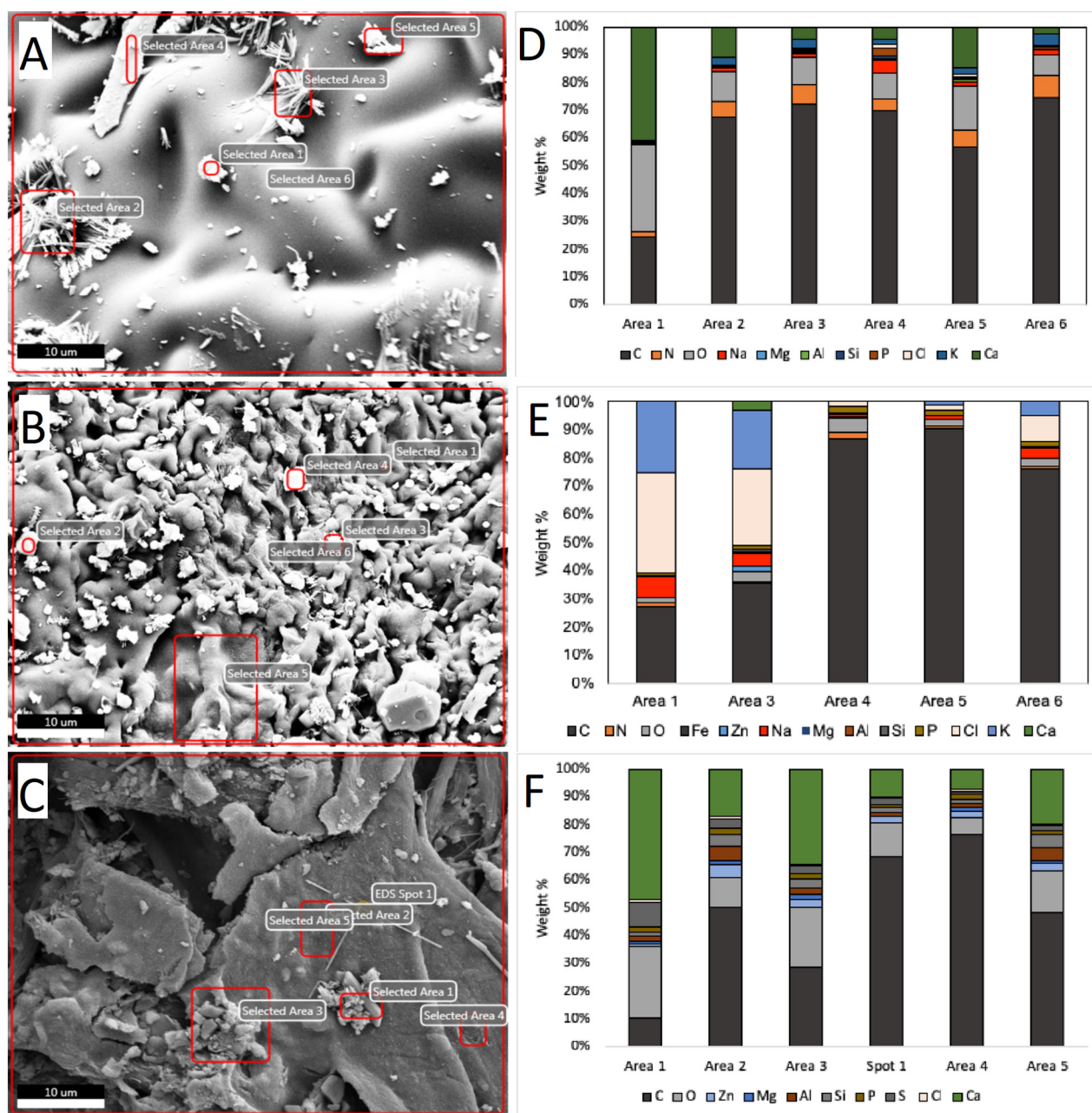
Fig. 4. SEM images of plastic char (A), food/organic char (B), and paper char (C) imaged at 5000× magnification with a working distance of 13–14 mm, and an electron energy of 10 kV before copper sorption, with elemental composition results for plastic, food/organic and paper chars shown in D, E and F, respectively.

These crystalline particles often contained greater weight percentages of minerals such as calcium, sodium, zinc and magnesium. Each different char contains minerals as a result of their presence in the precursor material (Schreiter et al., 2018).

Paper shows a lower weight % of carbon probably due to paper consisting predominantly of cellulose. Cellulose has a thermal decomposition temperature of 300–420 °C; in addition the thermal decomposition of most plastics occurs at temperatures generally in excess of 400 °C (Sophonrat et al., 2018). It has also been found that non pyrolyzed paper and plastic have carbon contents of 40–45% and 65–70% respectively (N. Yang et al., 2018). These values are very similar to the weight percentage of carbon found in paper and plastic char in this study. This suggests that the paper and plastic have not fully pyrolyzed at a pyrolysis temperature of 300 °C. Despite

this, paper is still shown to remove a similar amount of copper compared to the organic feedstock char.

SEM images of char analysed using EDAX after copper adsorption are shown in Fig. 5 A, B and C with D, E and F showing the copper weight % in each of the EDAX scans. The final bar on the right of the bar charts shown in Fig. 5 D–F shows the total area scan results which show plastic char having lower copper sorption than organic and paper char. This is possibly due to the reduced surface area of plastic char compared to the organic char. Plastic char SEM images revealed a smooth featureless surface indicating a low surface area when compared to the rougher surfaces of both paper and organic chars.

Calcium and other mineral content are commonly introduced to plastics as a filler material, therefore, mineral content present in
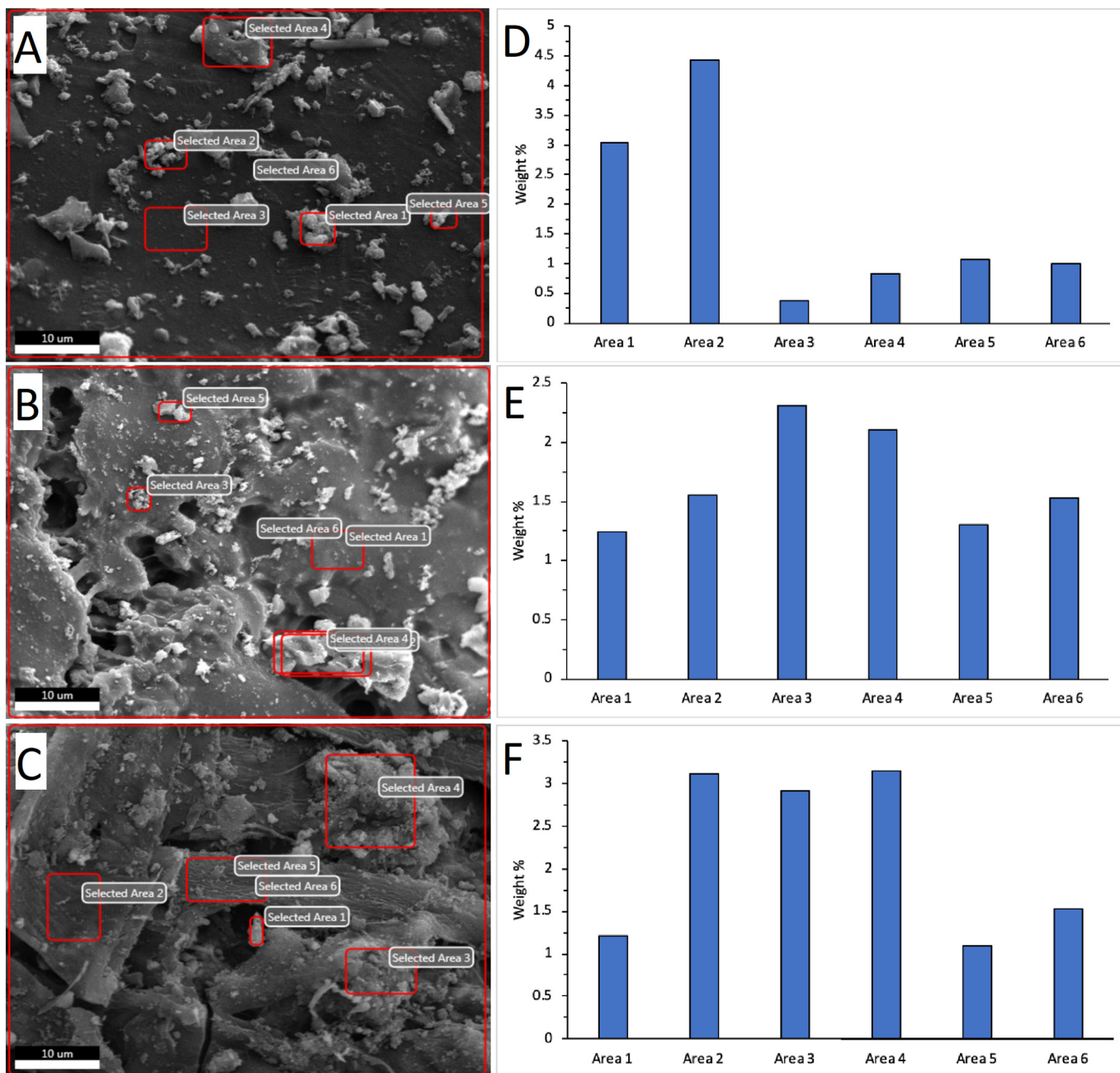
Fig. 5. SEM images of plastic char (A), food/organic char (B), and paper char (C) imaged at 5000× magnification with a working distance of 13–14 mm, and an electron energy of 10 kV. After copper sorption, percentage weight of copper for plastic, food/organic and paper chars shown in D, E and F, respectively.

the plastic char is likely due to the use of mineral compounds in conditioning the plastic during production (Ranta-Korpi et al., 2014).

3.2. FTIR

FTIR scans displayed in Fig. 6 A, B C and show the FTIR spectra for plastic, food/organic, and paper char, respectively. SEM-EDAX analysis displayed in Fig. 4 D and F show that as calcium content increases so does the oxygen content in plastic and paper chars. The relationship between Ca and O can be explained in the paper char as calcium carbonate is added as a filler to paper to improve its structure as well as its "brightness" (Seo et al., 2017). Indeed, the peaks at 873 cm^{-1} and 713 cm^{-1} indicate CO_3 presence (Djebaili et al., 2015), this peak is visible in all char types, but is most pronounced in the paper char FTIR scan (Gupta et al., 2018). However, these peaks may also suggest the presence of tri-

substituted benzene rings in the paper and organic char (W.-G. Li et al., 2018). The peak at 1423 cm^{-1} in both paper and organic chars denotes the presence of C=O and O—H bonds (Pereira et al., 2017), however, it may also suggest the presence of C—O—O stretches in the char (Kumar et al., 2018). The peak at 1030 cm^{-1} indicates the presence of kaolin in paper char. Kaolin is a chemical compound which is used in the production process of paper as it is used as a filler material (Bosch-Reig et al., 2017; Tartu, 2015). Fig. 6 A shows the FTIR spectrum for the plastic char which notably does not possess the strong 1423 cm^{-1} peak seen in food/organic and paper chars. The peak at 1241 cm^{-1} denotes the presence of amines in the plastic char (Tang et al., 2019), with the peak at 1576 cm^{-1} also showing the presence of amides. The peak at 1091 cm^{-1} suggests the presence of aliphatic ether C—O or alcoholic C—O, but could also suggest the presence of Si—O—Si bonds in the char (Nardon et al., 2014). Overall, the FTIR
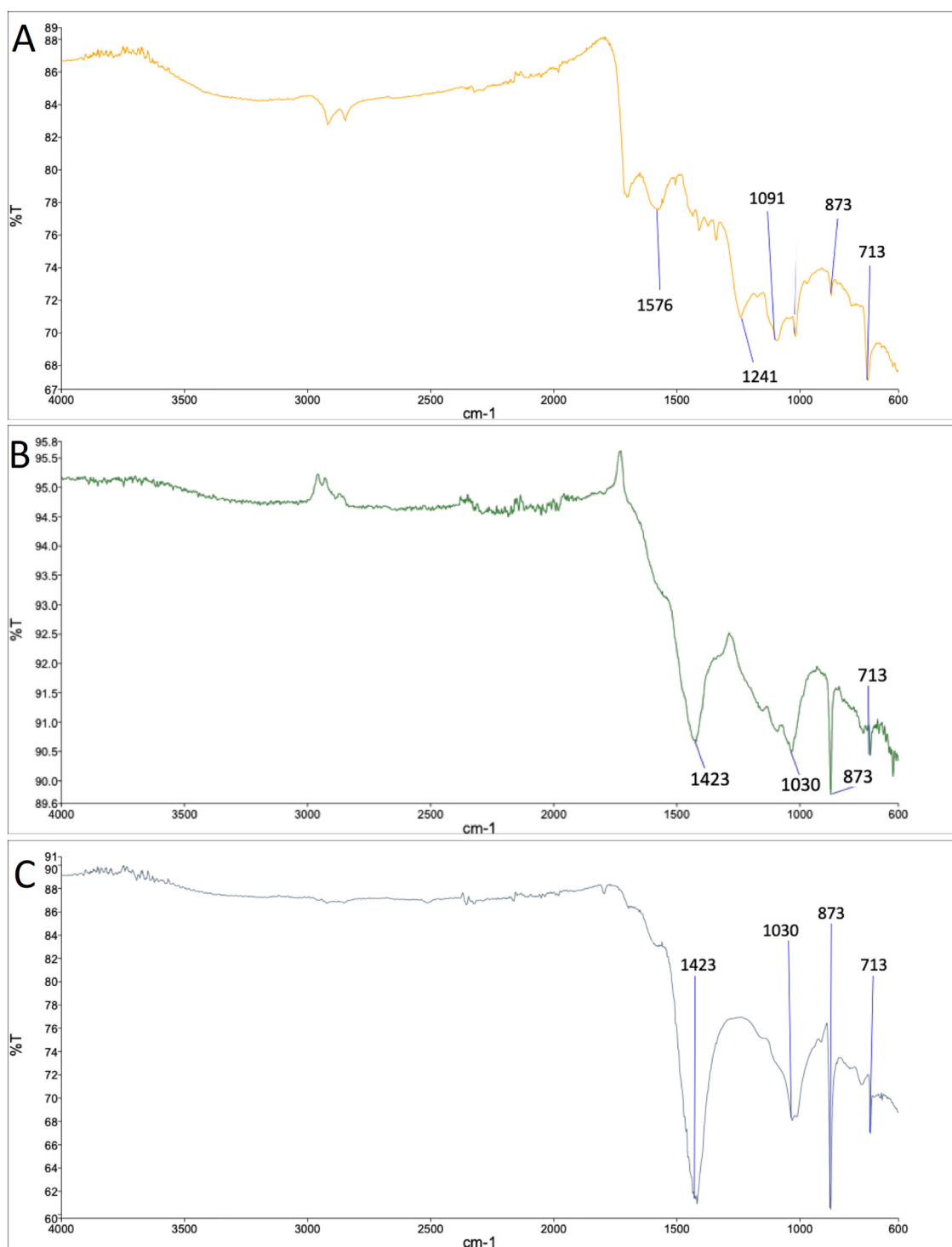
Fig. 6. FTIR analysis for plastic char (A), food/organic char (B), paper char (C), scanned between 4000 and 400 cm^{-1}.

results show paper and food/organic chars have similar characteristics, whereas plastic char has very different characteristics with the other two chars.

3.3. Sorption mechanisms

There are many sorption mechanisms by which copper is removed by char, these include complexation, adsorption, physical attraction (such as van der Waal's), and ion exchange. O/C ratio is thought to play a large role in the adsorption of copper and other metals to char

(Arán et al., 2016; Chen et al., 2011). Table 2 shows results of linear regression at 95% confidence level including p-values between collated positive ions, oxygen and negative ions and copper, collected using SEM/EDAX. Positive ions in the char include calcium, sodium, potassium, iron, aluminium, magnesium and zinc ions. Negative ions consisted of chlorine, phosphorous, and sulphur. Plastic char shows strong positive correlations for oxygen, and positive ions with copper, these being statistically significant with p-values below 0.05. This shows that ion exchange processes were largely responsible for aqueous copper removal in the plastic char.

Table 2
Linear regression results of positive ions, negative ions, oxygen compared against copper in char samples after adsorption from SEM/EDAX analysis.

	Plastic	Paper	Organic
Oxygen: copper			
Oxygen content range	6.14–25.12%	5.94–30.44%	6.96–10.86%
R^2	0.9681	0.41	0.1955
Coefficient	0.029	0.0152	0.1239
Intercept	−0.0772	0.3452	0.6409
p-Value	0.0024	0.1708	0.2562
Positive ions: copper			
Positive ions content range	0.92–13.06%	6.21–29.22%	4.94–9.29%
R^2	0.9855	0.2024	0.0094
Coefficient	0.047	0.014	0.0246
Intercept	0.0464	0.3279	1.5028
p-Value	0.0007	0.3707	0.7884
Negative ions: copper			
Negative ions content range	0.44–1.55%	0.88–2.71%	1.20–2.51%
R^2	0.8834	0.0904	0.1126
Coefficient	0.4983	0.1115	0.095
Intercept	−0.1349	0.3927	0.3426
p-Value	0.0175	0.5625	0.5155

Paper and food/organic chars show weak correlations and no statistical significance between copper and either positive ions/negative ions/oxygen. This indicates that processes other than ion exchange may have

a larger effect on the removal of copper from solution in paper and food/organic chars. Such processes may include surface complexation, physical attraction (van der Waal's), or the replacement of R-H groups with $R\text{-}Cu^+$ or R-Cu-OH groups (Li et al., 2017).

3.4. Adsorption kinetics

The results from the adsorption kinetics for all experimental conditions are shown in Fig. 7 with statistical analysis displayed in Table 3. Where $Q_{e,PSO}$ is the equilibrium adsorption according to the pseudo second order kinetic model, K_2 is the pseudo second order constant, R^2 is the coefficient of determination, $Q_{e,PFO}$ is the adsorption at equilibrium according to the pseudo first order kinetic model, K_1 is the pseudo first order constant. Notably, no sorption was observed below pH 3.5. In acidic conditions the surface groups are protonated. In addition, there is also competition between the hydronium and copper ions, thus resulting in free copper ions remaining in solution and a decreased sorption of copper to char (Cibati et al., 2017). At higher pH, the deprotonation of the surface groups means that char particles are more likely to have negatively charged sites, meaning more electro-static interaction with positively charged copper ions (Arán et al., 2016).

Another notable observation from Fig. 7 and Table 3 is the variation in some experiments. The experiment regarding 100 mg/L, at pH 5 shows a higher sorptive capacity when compared with other experimental conditions. It is possible that the char used in each of the
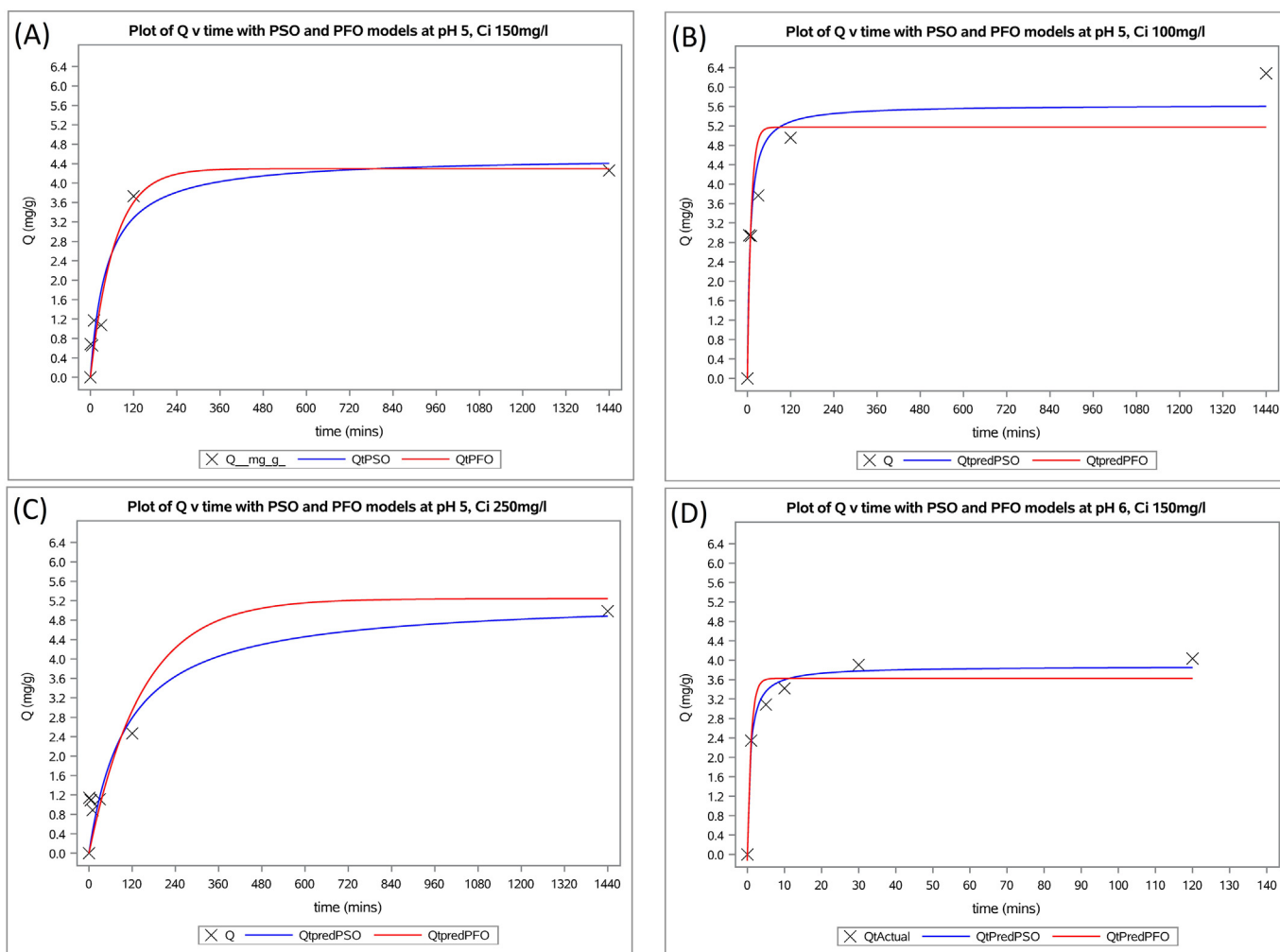

Fig. 7. (A) pH 5, initial concentration 150 mg/L; (B) pH 5, initial concentration 100 mg/L; (C) pH 5, initial concentration 250 mg/L; (D) pH 6, initial concentration 150 mg/L with blue lines showing pseudo second order kinetic model, and red lines showing pseudo first order kinetic model. (For interpretation of the references to colour in this figure legend, the reader is referred to the web version of this article.)

Table 3
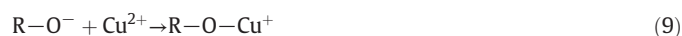The non-linear regression results for kinetic adsorption models compared with actual data.

Conditions	$Q_{e,PSO}$ (mg·g^{-1})	K_2 (g·mg^{-1}·min^{-1})	R^2	$Q_{e,PFO}$ (mg·g^{-1})	K_1 (min^{-1})	R^2
150 mg/L, pH 6 non-centrifuged initial solution	27.5571	0.6236	0.5406	27.3985	3.0752	0.5402
150 mg/L, pH 6 centrifuged initial solution	3.8726	0.3357	0.990	3.6249	1.0060	0.9692
150 mg/L, pH 5	4.5473	0.00475	0.933	4.2962	0.0152	0.9535
250 mg/L, pH 5	5.2404	0.00181	0.9264	4.9301	0.00685	0.9327
100 mg/L, pH 5	5.6321	0.0225	0.9279	5.1757	0.0976	0.8501

experiments had a slightly different composition of plastic, paper and organic chars. Different precursor materials have different conditions of pH at which they perform best as adsorbents, as well as different sorptive capacities (Keno et al., 2016).

The majority of the results in Table 3 show that the Pseudo second order kinetic model is the best fitting model for the sorption of copper to low temperature pyrolyzed MMDM across the experimental conditions used. An interesting result can be observed between 150 mg/L pH 5, and 150 mg/L pH 6 where there is an apparent decrease in sorption. Demirbas et al., 2009 had observed the precipitation of Cu(OH)$_2$ which started at pH 6 (Demirbas et al., 2009). The findings from the experiment carried out in this paper confirm this observation and the reduction of sorption capacity of Cu(II). To further investigate, the initial solution at pH 6 was centrifuged. Centrifuging the solution removed the copper hydroxide precipitate from the sample. Using AAS to analyse both the centrifuged supernatant of the initial solution and non-centrifuged initial solution it was found an aqueous copper concentration of around 30 mg/L was present in the supernatant of the centrifuged solution with the non-centrifuged solution still containing 150 mg/L of copper. The concentration was reduced to 10.9 mg/L over 120 min of stirring with char. The results derived from centrifuged initial solution reveal the actual copper adsorption to char to be 3.82 mg/g at an initial solution (pH 6 and initial concentration of 150 mg/L), with hydroxide precipitation being the principal process of copper removal. Meanwhile with the non-centrifuged samples (pH 6 and initial concentration of 150 mg/L) the copper removal was approximately seven-times higher. This is promising for industries that use alkaline solutions to precipitate heavy metals, as a low-cost char produced from municipal waste could also be added to these chemical treatment processes to assist in heavy metal removal thus reducing operating costs of chemical waste treatment facilities.

The reason for the increased sorption capacity at higher initial pH is potentially due to the increased presence of Cu(OH)$^+$ in solution (Zhou et al., 2019). The Cu(OH)$^+$ ion increases in amount to a maximum at

around pH 6. Then the concentration of Cu(OH)$^+$ decreases to 0 mol/l at around pH 8 (Albrecht et al., 2011). This ion exists in an equilibrium with Cu^{2+} seen in Eq. (7). As Cu(OH)$^+$ adsorbs to the char, the equilibrium shifts to replace the Cu(OH)$^+$, reducing the Cu^{2+} concentration. This mechanism could also result in the increased chemi-sorption capacity of the char, the Cu(OH)$^+$ ion only requires one negatively charged site, whereas the Cu^{2+} ion can occupy two closely situated negatively charged sites. Additionally, when the Cu^{2+} ion adsorbs to the char it may still possess a positive charge, potentially repelling other positively charged ions from adsorbing to active sites nearby. This is demonstrated in Eqs. (8), (9) and Eq. (10) where a deprotonated hydroxyl group represents an "active site". The Cu(OH)$^+$ ion thus increases the likelihood of sorption, and the capacity of the char to adsorb copper in solution (Jin et al., 2016; Albrecht et al., 2011).

$$Cu^{2+} + 2H_2O \rightleftharpoons Cu(OH)^+ + H_3O^+ \tag{7}$$

$$R-O^- + Cu(OH)^+ \rightarrow R-O-CuOH \tag{8}$$

$$R-O^- + Cu^{2+} \rightarrow R-O-Cu^+ \tag{9}$$

$$2(R-O^-) + Cu^{2+} \rightarrow 2(R-O)Cu \tag{10}$$

A common observation seen in experiments of high initial copper concentration (>100 mg/L) or low pH (<5) was a rapid removal of copper followed by an apparent desorption of copper. This phenomenon can be seen in Fig. 8. The initial rapid increase and subsequent decrease in sorption make the fit with the pseudo second and pseudo first order models less closely fitting to the data collected. This shows that the sorption of copper to pyrolyzed MMDM reaches a saturation point above the equilibrium point in these high initial concentrations, or low pH conditions (Adeyemo et al., 2014; Pillai et al., 2013). Fig. 8 also shows that the adsorption can increase past the initial decrease. This is not reported in literature as durations at which samples are taken for
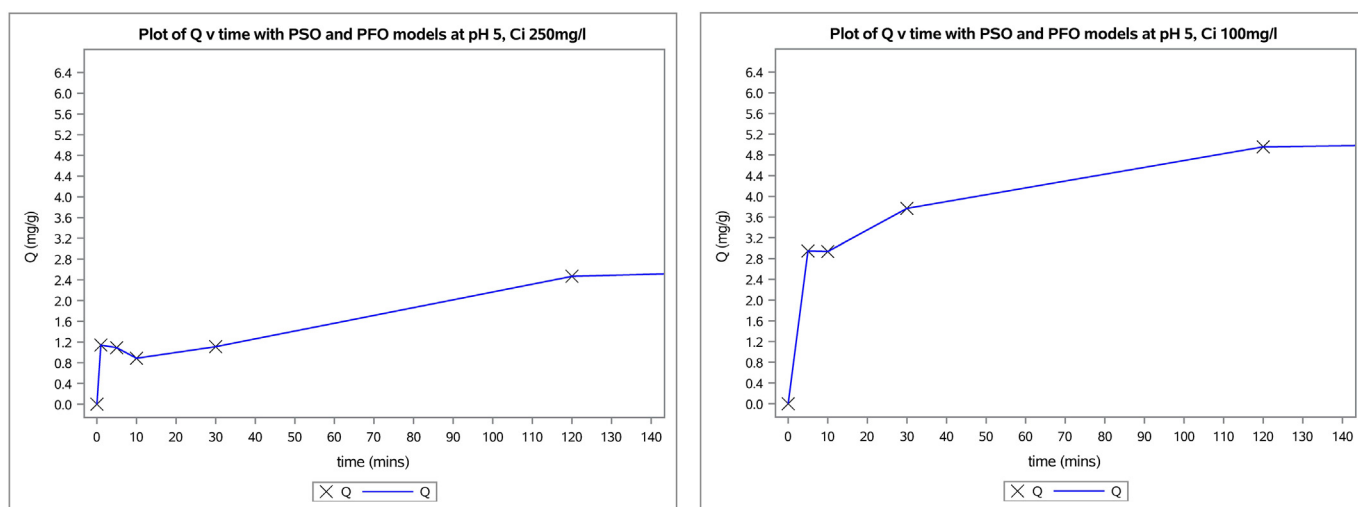

Fig. 8. Kinetics of copper desorption at higher concentration experiments; 250 mg/L and 100 mg/L (pH 5).

Table 4
Table showing adsorption isotherm models.

	Langmuir			Freundlich		
	K_L	Q_M	R^2	n	K_f	R^2
Linear regression method	0.123	4.144	0.8290	15.221	1.819	0.5792
Non-linear regression method	0.081	4.781	0.466	4.8643	1.5527	0.3887

kinetic studies are commonly in excess of 10 min after starting the agitation of copper solution with char (Batool et al., 2017; Jalayeri and Pepe, 2019; Shen et al., 2018; Xiao et al., 2017; Zhou et al., 2013). Further studies should therefore be conducted to determine the adsorption characteristics of copper to biochar in its initial stages during the first few minutes of contact.

3.5. Adsorption isotherms

Isothermal models describe the nature of sorption or an adsorbate-adsorbent interaction. The Langmuir model assumes monolayer adsorption, whereas the Freundlich model also allows for multi-layer adsorption. Table 4 shows the isothermal models assessed during this study, results from both the linear and non-linear methods are shown. Using the linear method for determining the isotherms, the Langmuir model was found to have the greatest R^2 value. The higher R^2 value in this case suggests that monolayer sorption has probably occurred. The low R^2 values in the isothermal models are probably due to the variation in feedstock material. Other studies on copper adsorption using char (Ahmad et al., 2018; Rodríguez-Vila et al., 2018) have found variations in Langmuir constants, maximum sorption capacities and R^2 values between different materials pyrolyzed at the same temperature. The materials in these studies are of similar origin being either manures or excess organic material, however they exhibit different isothermal characteristics despite the similarity. It can therefore be stated that the wide range of precursor materials in this study accounts for the poorer fits in the isothermal data.

3.6. Effect of pH on copper sorption to char

The effect of pH on copper sorption to char has been investigated. Fig. 9 shows the effect of initial solution pH on copper sorption to MMDM char. As initial solution pH increases from 3 to 5.5, the sorption of copper to char also increases. However, there is a decrease in copper sorption at pH 6. This can be explained due to the increased amount of

$Cu(OH)_2$ precipitate produced at higher pH, thus decreasing the availability of copper ions in solution. Results for pH 3 show apparent desorption of copper from the char, this is however unlikely as no significant trace of copper was detected in the SEM/EDAX scans before copper sorption.

A previous study regarding pH effects on copper adsorption to biochar showed that adsorption capacity plateaus as pH increases, with copper adsorption tending to plateau at around a pH of 5 (Goh et al., 2019). The same phenomenon was observed in this study where the inhibiting effects of H_3O^+ ions reduce the ability of char to adsorb copper at pH below 4.5. At pH >5.5 adsorption is reduced due to copper hydroxide precipitation becoming the major removal mechanism.

4. Discussion

4.1. Meaning and impact of results

To enable comprehensive discussion, Table 5 has been added to show results from similar studies regarding copper adsorption along with the findings from this paper. Clearly in literature there are chars that exhibit very high (>30 mg/g) copper adsorptions. These chars, however, tend to be produced using higher pyrolysis temperatures than in this study, and/or involve chemical activation steps as well. The table also shows that non-activated agricultural wastes pyrolyzed at the same temperature as in this study show similar adsorption amounts. This study observed that chars derived from food/organic waste had a higher adsorption of copper than chars derived from plastics under the same conditions. It is therefore possible that the MMDM char from the pyrolysis of domestic waste could exhibit a higher adsorption of copper if plastic is removed from the feedstock using the same pyrolysis conditions as those in the study on agricultural waste in Table 5 (Pellera et al., 2012). From the table it is noticeable that research tends to focus on the pyrolysis of specific feedstock rather than the mixture used in this study (Arán et al., 2016; Frišták et al., 2015; F. Yang et al., 2018; Zhou et al., 2017).

The purpose of this study is to investigate whether char produced from MMDM could be used to remove copper ions from solution without the need for chemical, steam, or temperature activation. The sorption performance of activated carbons for commercial use is far greater than the char in this work. Despite this, the results show that char for effective copper adsorption below an initial concentration of 100 mg/L with a solution pH >4.5 can be produced using MMDM and can be used effectively to reduce copper concentration. This indicates the potential use of simply produced char for copper removal in areas
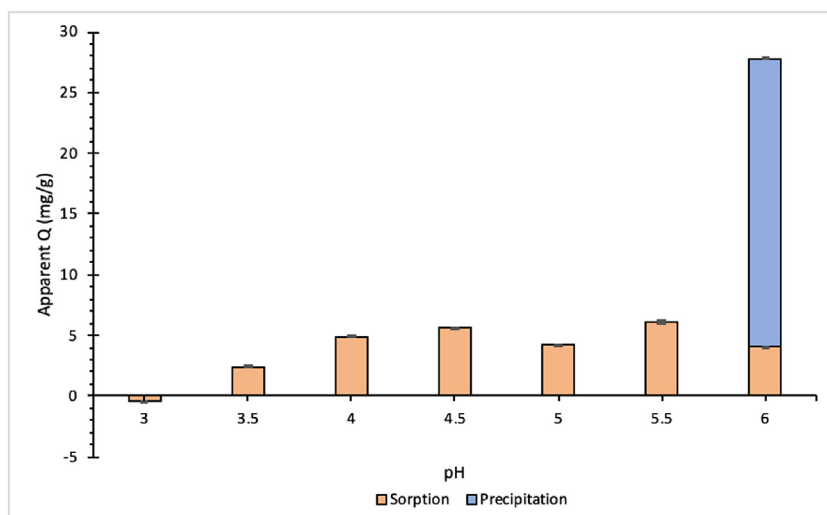

Fig. 9. Figure showing pH effect on copper sorption to char at initial concentration of 150 mg/L.

Table 5
Copper adsorption results from this study compared to copper adsorption results in similar studies.

Precursor material	Dosage (g/L)	Initial conc. (mg/L)	pH	Agitation time (min)	Adsorption (mg/g)	Source
Current study						
MMDM pyrolyzed at 300 °C for 12 h	5.00	50	5	1440	3.42	Current study
MMDM pyrolyzed at 300 °C for 12 h	5.00	100	5	1440	6.28	
MMDM pyrolyzed at 300 °C for 12 h	5.00	150	3.5	1440	2.44	
MMDM pyrolyzed at 300 °C for 12 h	5.00	150	4	1440	4.92	
MMDM pyrolyzed at 300 °C for 12 h	5.00	150	4.5	1440	5.15	
MMDM pyrolyzed at 300 °C for 12 h	5.00	150	5	1440	4.26	
MMDM pyrolyzed at 300 °C for 12 h	5.00	150	5.5	1440	6.08	
MMDM pyrolyzed at 300 °C for 12 h	5.00	150 (reduced to 30 by precipitation)	6	120	3.82	
Other studies						
Kelp, magnetised after pyrolysis	16.67	1200	Not specified	1440	69.35	(Son et al., 2018)
Hijikia, magnetised after pyrolysis	16.67	1200	Not specified	1440	67.43	(Son et al., 2018)
Rice straw, activated using ZnCl₂ prior to pyrolysis	0.4	140	5	1440	41.5	(Yin et al., 2018)
Giant Miscanthus pyrolyzed at 500 °C for 1+ h	2	150	6	2880	15.4	(Shim et al., 2015)
Rice straw pyrolyzed at 600 °C for 4 h	2	100	5	1440	42.1	(Park et al., 2017)
Anaerobically digested algae-dairy-manure slurry pyrolyzed at 400 °C for 30 min	2	400	6	1440	21.12	(Jin et al., 2016)
Hickory chips pyrolyzed at 600 °C for 2 h	1	100	5	1440	2.64	(Ding et al., 2016)
Rice husks pyrolyzed at 300 °C	5	50	5	120	4.6	(Pellera et al., 2012)
Olive pomace pyrolyzed at 300 °C	5	50	5	120	4.4	(Pellera et al., 2012)
Orange waste pyrolyzed at 300 °C	5	50	5	120	4.1	(Pellera et al., 2012)
Compost Pyrolyzed at 300 °C	5	50	5	120	7	(Pellera et al., 2012)

downstream of industries such as mining operations in developing countries, with the removal capacity of the MMDM char being shown to be around 4–5 mg/g between 50 and 100 mg/L.

The experiment using pH 6 saw the aqueous copper concentration reduction from 150 mg/L to 30 mg/L, with the MMDM char further reducing this to 10.9 mg/L. This shows that MMDM char may be applicable to drinking water filter applications in the developing world where poor waste management leads to degraded drinking water sources (da Silva et al., 2018; Idrees et al., 2018). The char may also be applicable in industrial waste water treatment, where it could be used as an additive to reduce the requirement of hydroxide for precipitation (Peligro et al., 2016), and thus operational costs in heavy metal removal. Pyrolyzed MMDM could also be applied to sustainable drainage and remediation systems where heavy metals in surface water discharge are increased by anthropogenic activities.

Discarded food and organic material represent a significant environmental issue, requiring large amounts of land and water for management. Additionally, food/organic waste contributes to CO_2 emissions, soil erosion and deforestation, in addition to the cost related to waste collection, transport to disposal sites, recycling and segregation (Jouhara et al., 2018). The previous study by Jouhara et al. (2018) focused on developed nations rather than developing nations. Data from the world bank group shows that food/organic material accounts for a higher proportion of MMDM in developing nations compared to developed nations (Group, 2012). It can be seen that pyrolysis processes used for waste management in developing nations could have a dramatic environmental impact. In terms of human health impact, pyrolyzing food/organic waste for use in household applications such as water filters could be very significant. Char is extensively researched for its adsorption capabilities and has shown favourable removal for a wide range of pollutants including pesticides, nitrates, heavy metals, pharmaceuticals and pathogens (Ding et al., 2016; Hass and Lima, 2018; Ozbay and Yargic, 2018; Satayeva et al., 2018; Son et al., 2018; Tan et al., 2015). If these can be effectively removed using char produced from local MMDM, profound health and environmental impacts are possible. Additionally, food waste attracts pests which can be a source of disease (Papargyropoulou et al., 2014), thus pyrolyzing discarded organic material could reduce illness due to waterborne contaminants like heavy metals as well as indirectly reducing diseases spread by rodents and other pests.

5. Conclusion

This article focused on the use of MMDM char as an adsorbent for the developing world, specifically towards its use in a decentralised drinking water application for the removal of copper ions from water. The results show that char produced from mixed feedstocks can be used successfully to remove copper from aqueous solutions. Maximum sorption capacity of low temperature ($\approx$300 °C) MMDM chars is shown to be 4–5 mg/g in the initial copper concentration range of 50–100 mg/L. The correlation with kinetic and isothermal models was affected by the variation in amounts of plastic, organic, and paper chars in the MMDM samples used for sorption, where each of these precursor materials produces chars of different characteristics. Plastic char exhibited high correlation between positive ions at the char surface and copper in SEM/EDAX scans, whereas paper and organic chars showed less localised concentrations of copper, indicating a difference in copper removal mechanisms between plastic, organic and paper chars. Further work before the char is used in a decentralised drinking water application should focus on any potential leaching of harmful polycyclic aromatic hydrocarbons (PAHs) and Dioxins from the char. Additional work may also include the removal of organic contaminants such as pesticides using a char of a similar nature to the char used in this study.

Acknowledgment

References

Abdelhadi, S.O., Dosoretz, C.G., Rytwo, G., Gerchman, Y., Azaizeh, H., 2017. Production of biochar from olive mill solid waste for heavy metal removal. Bioresour. Technol. 244, 759–767. https://doi.org/10.1016/j.biortech.2017.08.013.

Adeyemo, A.O., Adebowale, K.O., B.I.O.-O, 2014. Adsorption of copper by biochar. Int. Res. J. Pure Appl. Chem. 4, 727–736. https://doi.org/10.9734/IRJPAC/2014/11079.

Ahmad, Z., Gao, B., Mosa, A., Yu, H., Yin, X., Bashir, A., Ghoveisi, H., Wang, S., 2018. Removal of Cu(II), Cd(II) and Pb(II) ions from aqueous solutions by biochars derived from potassium-rich biomass. J. Clean. Prod. 180, 437–449. https://doi.org/10.1016/j.jclepro.2018.01.133.

Albrecht, T.W.J., Addai-Mensah, J., Fornasiero, D., 2011. Effect of pH, concentration and temperature on copper and zinc hydroxide formation/precipitation in solution. CHEMECA 2011 - "Engineering a Better World".

Al-Malack, M.H., Dauda, M., 2017. Competitive adsorption of cadmium and phenol on activated carbon produced from municipal sludge. J. Environ. Chem. Eng. 5, 2718–2729. https://doi.org/10.1016/j.jece.2017.05.027.

Al-Saydeh, S.A., El-Naas, M.H., Zaidi, S.J., 2017. Copper removal from industrial wastewater: a comprehensive review. J. Ind. Eng. Chem. 56, 35–44. https://doi.org/10.1016/j.jiec.2017.07.026.

Arán, D., Antelo, J., Fiol, S., Macías, F., 2016. Influence of feedstock on the copper removal capacity of waste-derived biochars. Bioresour. Technol. 212, 199–206. https://doi.org/10.1016/j.biortech.2016.04.043.

Balasundram, V., Ibrahim, N., Kasmani, R.M., Hamid, M.K.A., Isha, R., Hasbullah, H., Ali, R.R., 2017. Thermogravimetric catalytic pyrolysis and kinetic studies of coconut copra and rice husk for possible maximum production of pyrolysis oil. J. Clean. Prod. 167, 218–228. https://doi.org/10.1016/j.jclepro.2017.08.173.

Batool, S., Idrees, M., Hussain, Q., Kong, J., 2017. Adsorption of copper (II) by using derived-farmyard and poultry manure biochars: efficiency and mechanism. Chem. Phys. Lett. 689, 190–198. https://doi.org/10.1016/j.cplett.2017.10.016.

Bosch-Reig, F., Gimeno-Adelantado, J.V., Bosch-Mossi, F., Doménech-Carbó, A., 2017. Quantification of minerals from ATR-FTIR spectra with spectral interferences using the MRC method. Spectrochim. Acta Part A Mol. Biomol. Spectrosc. 181, 7–12. https://doi.org/10.1016/j.saa.2017.02.012.

Chen, X., Chen, G., Chen, L., Chen, Y., Lehmann, J., McBride, M.B., Hay, A.G., 2011. Adsorption of copper and zinc by biochars produced from pyrolysis of hardwood and corn straw in aqueous solution. Bioresour. Technol. 102, 8877–8884. https://doi.org/10.1016/j.biortech.2011.06.078.

Cibati, A., Foereid, B., Bissessur, A., Hapca, S., 2017. Assessment of Miscanthus × giganteus derived biochar as copper and zinc adsorbent: study of the effect of pyrolysis temperature, pH and hydrogen peroxide modification. J. Clean. Prod. 162, 1285–1296. https://doi.org/10.1016/j.jclepro.2017.06.114.

Da'na, E., Awad, A., 2017. Regeneration of spent activated carbon obtained from home filtration system and applying it for heavy metals adsorption. J. Environ. Chem. Eng. 5, 3091–3099. https://doi.org/10.1016/j.jece.2017.06.022.

Demirbas, E., Dizge, N., Sulak, M.T., Kobya, M., 2009. Adsorption kinetics and equilibrium of copper from aqueous solutions using hazelnut shell activated carbon. Chem. Eng. J. 148, 480–487. https://doi.org/10.1016/j.cej.2008.09.027.

Ding, Z., Hu, X., Wan, Y., Wang, S., Gao, B., 2016. Removal of lead, copper, cadmium, zinc, and nickel from aqueous solutions by alkali-modified biochar: batch and column tests. J. Ind. Eng. Chem. 33, 239–245. https://doi.org/10.1016/j.jiec.2015.10.007.

Djebaili, K., Mekhalif, Z., Djelloul, A., 2015. XPS, FTIR, EDX, and XRD analysis of Al2O3 scales grown on PM2000 alloy. J. Spectrosc. 2015. https://doi.org/10.1155/2015/868109.

El Maguana, Y., Elhadiri, N., Bouchdoug, M., Benchanaa, M., 2018. Study of the influence of some factors on the preparation of activated carbon from walnut cake using the fractional factorial design. J. Environ. Chem. Eng. 6, 1093–1099. https://doi.org/10.1016/j.jece.2018.01.023.

Enniya, I., Rghioui, L., Jourani, A., 2018. Adsorption of hexavalent chromium in aqueous solution on activated carbon prepared from apple peels. Sustain. Chem. Pharm. 7, 9–16. https://doi.org/10.1016/j.scp.2017.11.003.

Frišták, V., Friesl-Hanl, W., Wawra, A., Pipíška, M., Soja, G., 2015. Effect of biochar artificial ageing on Cd and Cu sorption characteristics. J. Geochemical Explor. 159, 178–184. https://doi.org/10.1016/j.gexplo.2015.09.006.

Goh, C.L., Sethupathi, S., Bashir, M.J.K., Ahmed, W., 2019. Adsorptive behaviour of palm oil mill sludge biochar pyrolyzed at low temperature for copper and cadmium removal. J. Environ. Manag. 237, 281–288. https://doi.org/10.1016/j.jenvman.2018.12.103.

González-García, P., 2018. Activated carbon from lignocellulosics precursors: a review of the synthesis methods, characterization techniques and applications. Renew. Sust. Energ. Rev. 82, 1393–1414. https://doi.org/10.1016/j.rser.2017.04.117.

Group, W.B, 2012. Waste composition. [WWW Document]. URL. http://siteresources.worldbank.org/INTURBANDEVELOPMENT/Resources/336387-1334852610766/Chap5.pdf.

Gunatilake, S.K., 2015. Methods of removing heavy metals from industrial wastewater. J. Multidiscip. Eng. Sci. Stud. 1, 12–18.

Gupta, A., Thengane, S.K., Mahajani, S., 2018. CO2 gasification of char from lignocellulosic garden waste: experimental and kinetic study. Bioresour. Technol. 263, 180–191. https://doi.org/10.1016/j.biortech.2018.04.097.

Hass, A., Lima, I.M., 2018. Effect of feed source and pyrolysis conditions on properties and metal sorption by sugarcane biochar. Environ. Technol. Innov. 10, 16–26. https://doi.org/10.1016/j.eti.2018.01.007.

Ho, S.-H., Chen, Y., Yang, Z., Nagarajan, D., Chang, J.-S., Ren, N., 2017. High-efficiency removal of lead from wastewater by biochar derived from anaerobic digestion sludge. Bioresour. Technol. 246, 142–149. https://doi.org/10.1016/j.biortech.2017.08.025.

Idrees, M., Batool, S., Kalsoom, T., Yasmeen, S., Kalsoom, A., Raina, S., Zhuang, Q., Kong, J., 2018. Animal manure-derived biochars produced via fast pyrolysis for the removal of divalent copper from aqueous media. J. Environ. Manag. 213, 109–118. https://doi.org/10.1016/j.jenvman.2018.02.003.

Jalayeri, H., Pepe, F., 2019. Novel and high-performance biochar derived from pistachio green hull biomass: production, characterization, and application to Cu(II) removal from aqueous solutions. Ecotoxicol. Environ. Saf. 168, 64–71. https://doi.org/10.1016/j.ecoenv.2018.10.058.

Jin, H., Hanif, M.U., Capareda, S., Chang, Z., Huang, H., Ai, Y., 2016. Copper(II) removal potential from aqueous solution by pyrolysis biochar derived from anaerobically digested algae-dairy-manure and effect of KOH activation. J. Environ. Chem. Eng. 4, 365–372. https://doi.org/10.1016/j.jece.2015.11.022.

Jouhara, H., Czajczyńska, D., Ghazal, H., Krzyżyńska, R., Anguilano, L., Reynolds, A.J., Spencer, N., 2017. Municipal waste management systems for domestic use. Energy 139, 485–506. https://doi.org/10.1016/j.energy.2017.07.162.

Jouhara, H., Ahmad, D., Czajczyńska, D., Ghazal, H., Anguilano, L., Reynolds, A., Rutkowski, P., Krzyżyńska, R., Katsou, E., Simons, S., Spencer, N., 2018. Experimental investigation on the chemical characterisation of pyrolytic products of discarded food at temperatures up to 300 °C. Therm. Sci. Eng. Prog. 5, 579–588. https://doi.org/10.1016/j.tsep.2018.02.010.

Kaçan, E., Kütahyalı, C., 2012. Adsorption of strontium from aqueous solution using activated carbon produced from textile sewage sludges. J. Anal. Appl. Pyrolysis 97, 149–157. https://doi.org/10.1016/j.jaap.2012.06.006.

Keno, D., Mauti, G., Mbaka, E., David Kowanga, K., Gatebe, E., Godfrey, O., Mauti, M., 2016. Correspondence: Kinetic, Sorption Isotherms, Pseudo-First-Order Model and Pseudo-Second-Order Model Studies of Cu(II) and Pb(II) Using Defatted Moringa oleifera Seed Powder.

Kumar, V., Ganesapillai, M., 2017. Preparation of activated carbon from municipal organic solid wastes. Mater. Today Proc. 4, 10648–10652. https://doi.org/10.1016/j.matpr.2017.06.436.

Kumar, A., Joseph, S., Tsechansky, L., Privat, K., Schreiter, I.J., Schüth, C., Graber, E.R., 2018. Biochar aging in contaminated soil promotes Zn immobilization due to changes in biochar surface structural and chemical properties. Sci. Total Environ. 626, 953–961. https://doi.org/10.1016/j.scitotenv.2018.01.157.

Li, H., Dong, X., da Silva, E.B., de Oliveira, L.M., Chen, Y., Ma, L.Q., 2017. Mechanisms of metal sorption by biochars: biochar characteristics and modifications. Chemosphere 178, 466–478. https://doi.org/10.1016/j.chemosphere.2017.03.072.

Li, J., Xing, X., Li, J., Shi, M., Lin, A., Xu, C., Zheng, J., Li, R., 2018a. Preparation of thiol-functionalized activated carbon from sewage sludge with coal blending for heavy metal removal from contaminated water. Environ. Pollut. 234, 677–683. https://doi.org/10.1016/j.envpol.2017.11.102.

Li, W.-G., Zhao, W., Liu, H.-M., Ao, L., Liu, K.-S., Guan, Y.-S., Zai, S.-F., Chen, S.-L., Zong, Z.-M., Wei, X.-Y., 2018b. Supercritical ethanolysis of wheat stalk over calcium oxide. Renew. Energy 120, 300–305. https://doi.org/10.1016/j.renene.2017.12.078.

Lin, J., Wang, L., 2009. Comparison between linear and non-linear forms of pseudo-first-order and pseudo-second-order adsorption kinetic models for the removal of methylene blue by activated carbon. Front. Environ. Sci. Eng. China 3, 320–324. https://doi.org/10.1007/s11783-009-0030-7.

Lone, M.I., He, Z., Stoffella, P.J., Yang, X., 2008. Phytoremediation of heavy metal polluted soils and water: progresses and perspectives. J Zhejiang Univ Sci B 9, 210–220. https://doi.org/10.1631/jzus.B0710633.

Luo, M., Lin, H., Li, B., Dong, Y., He, Y., Wang, L., 2018. A novel modification of lignin on corncob-based biochar to enhance removal of cadmium from water. Bioresour. Technol. 259, 312–318. https://doi.org/10.1016/j.biortech.2018.03.075.

Marques, S.C.R., Mestre, A.S., Machuqueiro, M., Gotvajn, A.Ž., Marinšek, M., Carvalho, A.P., 2018. Apple tree branches derived activated carbons for the removal of β-blocker atenolol. Chem. Eng. J. https://doi.org/10.1016/j.cej.2018.01.076.

Menya, E., Olupot, P.W., Storz, H., Lubwama, M., Kiros, Y., 2018a. Production and performance of activated carbon from rice husks for removal of natural organic matter from water: a review. Chem. Eng. Res. Des. 129, 271–296. https://doi.org/10.1016/j.cherd.2017.11.008.

Menya, E., Olupot, P.W., Storz, H., Lubwama, M., Kiros, Y., 2018b. Characterization and alkaline pretreatment of rice husk varieties in Uganda for potential utilization as precursors in the production of activated carbon and other value-added products. Waste Manag. 81, 104–116. https://doi.org/10.1016/j.wasman.2018.09.050.

Momčilović, M., Purenović, M., Bojić, A., Zarubica, A., Ranđelović, M., 2011. Removal of lead(II) ions from aqueous solutions by adsorption onto pine cone activated carbon. Desalination 276, 53–59. https://doi.org/10.1016/j.desal.2011.03.013.

Moreira, M.T., Noya, I., Feijoo, G., 2017. The prospective use of biochar as adsorption matrix – a review from a lifecycle perspective. Bioresour. Technol. 246, 135–141. https://doi.org/10.1016/j.biortech.2017.08.041.

Nardon, C., W., S., Ahmad Husni, M., Mohd Amran, M., 2014. Effects of pyrolysis temperature on the physicochemical properties of empty fruit bunch and rice husk biochars. Waste Manag. Res. J. Int. Solid Wastes Public Cleansing Assoc. ISWA https://doi.org/10.1177/0734242X14525822.

National Research Council, U. (Committee on C. in D.W.), 2000. Health effects of excess copper. Copper in Drinking Water (Washington DC).

Ozbay, N., Yargic, A.S., 2018. Statistical analysis of Cu(II) and Co(II) sorption by apple pulp carbon using factorial design approach. J. Ind. Eng. Chem. 57, 275–283. https://doi.org/10.1016/j.jiec.2017.08.033.

Pan, J., Ma, J., Liu, X., Zhai, L., Ouyang, X., Liu, H., 2019. Effects of different types of biochar on the anaerobic digestion of chicken manure. Bioresour. Technol. 275, 258–265. https://doi.org/10.1016/j.biortech.2018.12.068.

Papargyropoulou, E., Lozano, R.K., Steinberger, J., Wright, N., Ujang, Z. bin, 2014. The food waste hierarchy as a framework for the management of food surplus and food waste. J. Clean. Prod. 76, 106–115. https://doi.org/10.1016/j.jclepro.2014.04.020.

Park, J.-H., Wang, J.J., Kim, S.-H., Cho, J.-S., Kang, S.-W., Delaune, R.D., Han, K.-J., Seo, D.-C., 2017. Recycling of rice straw through pyrolysis and its adsorption behaviors for Cu and Zn ions in aqueous solution. Colloids Surf. A Physicochem. Eng. Asp. 533, 330–337. https://doi.org/10.1016/j.colsurfa.2017.08.041.

Peligro, F.R., Pavlovic, I., Rojas, R., Barriga, C., 2016. Removal of heavy metals from simulated wastewater by in situ formation of layered double hydroxides. Chem. Eng. J. 306, 1035–1040. https://doi.org/10.1016/j.cej.2016.08.054.

Pellera, F.-M., Giannis, A., Kalderis, D., Anastasiadou, K., Stegmann, R., Wang, J.-Y., Gidarakos, E., 2012. Adsorption of Cu(II) ions from aqueous solutions on biochars prepared from agricultural by-products. J. Environ. Manag. 96, 35–42. https://doi.org/10.1016/j.jenvman.2011.10.010.

Pereira, A.P. dos S., Silva, M.H.P. da, Lima Júnior, É.P., Paula, A. dos S., Tommasini, F.J., Pereira, A.P. dos S., Silva, M.H.P. da, Lima Júnior, É.P., Paula, A. dos S., Tommasini, F.J., 2017. Processing and characterization of PET composites reinforced with

geopolymer concrete waste. Mater. Res. 20, 411–420. https://doi.org/10.1590/1980-5373-mr-2017-0734.

Pillai, S.S., Deepa, B., Abraham, E., Girija, N., Geetha, P., Jacob, L., Koshy, M., 2013. Biosorption of Cd(II) from aqueous solution using xanthated nano banana cellulose: equilibrium and kinetic studies. Ecotoxicol. Environ. Saf. 98, 352–360. https://doi.org/10.1016/j.ecoenv.2013.09.003.

Poo, K.-M., Son, E.-B., Chang, J.-S., Ren, X., Choi, Y.-J., Chae, K.-J., 2018. Biochars derived from wasted marine macro-algae (Saccharina japonica and Sargassum fusiforme) and their potential for heavy metal removal in aqueous solution. J. Environ. Manag. 206, 364–372. https://doi.org/10.1016/j.jenvman.2017.10.056.

Qian, L., Zhang, W., Yan, J., Han, L., Gao, W., Liu, R., Chen, M., 2016. Effective removal of heavy metal by biochar colloids under different pyrolysis temperatures. Bioresour. Technol. 206, 217–224. https://doi.org/10.1016/j.biortech.2016.01.065.

Ranta-Korpi, M., Vainikka, P., Konttinen, J., Saarimaa, A., Rodriguez, M., 2014. Ash Forming Elements in Plastics and Rubbers.

Rashidi, N.A., Yusup, S., 2017. Potential of palm kernel shell as activated carbon precursors through single stage activation technique for carbon dioxide adsorption. J. Clean. Prod. 168, 474–486. https://doi.org/10.1016/j.jclepro.2017.09.045.

Rodríguez-Vila, A., Selwyn-Smith, H., Enunwa, L., Smail, I., Covelo, E.F., Sizmur, T., 2018. Predicting Cu and Zn sorption capacity of biochar from feedstock C/N ratio and pyrolysis temperature. Environ. Sci. Pollut. Res. Int. 25, 7730–7739. https://doi.org/10.1007/s11356-017-1047-2.

Satayeva, A.R., Howell, C.A., Korobeinyk, A.V., Jandosov, J., Inglezakis, V.J., Mansurov, Z.A., Mikhalovsky, S.V., 2018. Investigation of rice husk derived activated carbon for removal of nitrate contamination from water. Sci. Total Environ. 630, 1237–1245. https://doi.org/10.1016/j.scitotenv.2018.02.329.

Schreiter, I.J., Schmidt, W., Schüth, C., 2018. Sorption mechanisms of chlorinated hydrocarbons on biochar produced from different feedstocks: conclusions from single- and bi-solute experiments. Chemosphere 203, 34–43. https://doi.org/10.1016/j.chemosphere.2018.03.173.

Seo, Y.B., Ahn, J.H., Lee, H.L., 2017. Upgrading waste paper by in-situ calcium carbonate formation. J. Clean. Prod. 155, 212–217. https://doi.org/10.1016/j.jclepro.2016.09.003.

Shen, T., Tang, Y., Lu, X.-Y., Meng, Z., 2018. Mechanisms of copper stabilization by mineral constituents in sewage sludge biochar. J. Clean. Prod. 193, 185–193. https://doi.org/10.1016/j.jclepro.2018.05.071.

Shim, T., Yoo, J., Ryu, C., Park, Y.-K., Jung, J., 2015. Effect of steam activation of biochar produced from a giant Miscanthus on copper sorption and toxicity. Bioresour. Technol. 197, 85–90. https://doi.org/10.1016/j.biortech.2015.08.055.

da Silva, A.J.F., de Alencar Moura, M.C.P., da Silva Santos, E., Saraiva Pereira, J.E., de Barros Neto, E.L., 2018. Copper removal using carnauba straw powder: equilibrium, kinetics, and thermodynamic studies. J. Environ. Chem. Eng. https://doi.org/10.1016/j.jece.2018.10.028.

Singh, R., Gautam, N., Mishra, A., Gupta, R., 2011. Heavy metals and living systems: an overview. Indian J. Pharmacol. 43, 246–253. https://doi.org/10.4103/0253-7613.81505.

Son, E.-B., Poo, K.-M., Chang, J.-S., Chae, K.-J., 2018. Heavy metal removal from aqueous solutions using engineered magnetic biochars derived from waste marine macro-algal biomass. Sci. Total Environ. 615, 161–168. https://doi.org/10.1016/j.scitotenv.2017.09.171.

Sophonrat, N., Sandström, L., Zaini, I.N., Yang, W., 2018. Stepwise pyrolysis of mixed plastics and paper for separation of oxygenated and hydrocarbon condensates. Appl. Energy 229, 314–325. https://doi.org/10.1016/j.apenergy.2018.08.006.

Spahis, N., Addoun, A., Mahmoudi, H., Ghaffour, N., 2008. Purification of water by activated carbon prepared from olive stones. Desalination 222, 519–527. https://doi.org/10.1016/j.desal.2007.02.065.

Tan, X., Liu, Y., Zeng, G., Wang, X., Hu, X., Gu, Y., Yang, Z., 2015. Application of biochar for the removal of pollutants from aqueous solutions. Chemosphere 125, 70–85. https://doi.org/10.1016/j.chemosphere.2014.12.058.

Tang, Y., Alam, M.S., Konhauser, K.O., Alessi, D.S., Xu, S., Tian, W., Liu, Y., 2019. Influence of pyrolysis temperature on production of digested sludge biochar and its application for ammonium removal from municipal wastewater. J. Clean. Prod. 209, 927–936. https://doi.org/10.1016/j.jclepro.2018.10.268.

Tartu, I. of C.U. of, 2015. ATR-FT-IR spectra of kaolinite ($Al_2O_3 \cdot 2SiO_2 \cdot 2H_2O$). [WWW Document]. URL http://lisa.chem.ut.ee/IR_spectra/paint/fillers/kaolinite/, Accessed date: 15 November 2018.

Wu, J., Montes, V., Virla, L.D., Hill, J.M., 2018. Impacts of amount of chemical agent and addition of steam for activation of petroleum coke with KOH or NaOH. Fuel Process. Technol. 181, 53–60. https://doi.org/10.1016/j.fuproc.2018.09.018.

Xiao, Y., Xue, Y., Gao, F., Mosa, A., 2017. Sorption of heavy metal ions onto crayfish shell biochar: effect of pyrolysis temperature, pH and ionic strength. J. Taiwan Inst. Chem. Eng. 80, 114–121. https://doi.org/10.1016/j.jtice.2017.08.035.

Yang, N., Damgaard, A., Scheutz, C., Shao, L.-M., He, P.-J., 2018a. A comparison of chemical MSW compositional data between China and Denmark. J. Environ. Sci. 74, 1–10. https://doi.org/10.1016/j.jes.2018.02.010.

Yang, F., Zhang, S., Li, H., Li, S., Cheng, K., Li, J.-S., Tsang, D.C.W., 2018b. Corn straw-derived biochar impregnated with α-FeOOH nanorods for highly effective copper removal. Chem. Eng. J. 348, 191–201. https://doi.org/10.1016/j.cej.2018.04.161.

Yin, Z., Liu, Y., Liu, S., Jiang, L., Tan, X., Zeng, G., Li, M., Liu, S., Tian, S., Fang, Y., 2018. Activated magnetic biochar by one-step synthesis: enhanced adsorption and coadsorption for 17β-estradiol and copper. Sci. Total Environ. 639, 1530–1542. https://doi.org/10.1016/j.scitotenv.2018.05.130.

Zhang, H., Chen, C., Gray, E.M., Boyd, S.E., 2017. Effect of feedstock and pyrolysis temperature on properties of biochar governing end use efficacy. Biomass Bioenergy 105, 136–146. https://doi.org/10.1016/j.biombioe.2017.06.024.

Zhou, Y., Gao, B., Zimmerman, A.R., Fang, J., Sun, Y., Cao, X., 2013. Sorption of heavy metals on chitosan-modified biochars and its biological effects. Chem. Eng. J. 231, 512–518. https://doi.org/10.1016/j.cej.2013.07.036.

Zhou, Y., Liu, X., Xiang, Y., Wang, P., Zhang, J., Zhang, F., Wei, J., Luo, L., Lei, M., Tang, L., 2017. Modification of biochar derived from sawdust and its application in removal of tetracycline and copper from aqueous solution: adsorption mechanism and modelling. Bioresour. Technol. 245, 266–273. https://doi.org/10.1016/j.biortech.2017.08.178.

Zhou, Y., He, Y., Xiang, Y., Meng, S., Liu, X., Yu, J., Yang, J., Zhang, J., Qin, P., Luo, L., 2019. Single and simultaneous adsorption of pefloxacin and Cu(II) ions from aqueous solutions by oxidized multiwalled carbon nanotube. Sci. Total Environ. 646, 29–36. https://doi.org/10.1016/j.scitotenv.2018.07.267.